Title

Achieving High-Accuracy Intermolecular Interactions by Combining Coulomb-Attenuated Second-Order Møller–Plesset Perturbation Theory with Coupled Kohn–Sham Dispersion

Journal

Journal of Chemical Theory and Computation, 10(5)

ISSN

1549-9618

Authors

Huang, Yuanhang
Goldey, Matthew
Head-Gordon, Martin
et al.

Publication Date

2014-05-13

DOI

10.1021/ct5002329

Peer reviewed

Achieving high-accuracy intermolecular interactions by combining Coulomb-attenuated second-order Møller-Plesset perturbation theory with coupled Kohn-Sham dispersion

Journal:	*Journal of Chemical Theory and Computation*
Manuscript ID:	ct-2014-002329.R1
Manuscript Type:	Article
Date Submitted by the Author:	17-Apr-2014
Complete List of Authors:	Huang, Yuanhang; University of Californa Riverside, Department of Chemistry Goldey, Matthew; University of California, Berkeley, College of Chemistry Head-Gordon, Martin; University of California, Berkeley, Chemistry; University of California, Berkeley, College of Chemistry Beran, Gregory; University of California at Riverside, Chemistry

Achieving high-accuracy intermolecular interactions by combining Coulomb-attenuated second-order Møller-Plesset perturbation theory with coupled Kohn-Sham dispersion

Yuanhang Huang,[†] Matthew Goldey,[‡] Martin Head-Gordon,[‡] and Gregory J. O. Beran[*,†]

Department of Chemistry, University of California, Riverside, California 92521 USA, and Department of Chemistry, University of California, Berkeley, California 94720 USA and Chemical Sciences Division, Lawrence Berkeley National Laboratory, Berkeley, California 94720, USA

E-mail: gregory.beran@ucr.edu

April 17, 2014

Abstract

The dispersion-corrected second-order Møller-Plesset perturbation theory (MP2C) approach accurately describes intermolecular interactions in many systems. MP2C, however, expends much computational effort to compute the long-range correlation with MP2, only to discard

[*]To whom correspondence should be addressed

[†]Department of Chemistry, University of California, Riverside, California 92521 USA

[‡]Department of Chemistry, University of California, Berkeley, California 94720 USA and Chemical Sciences Division, Lawrence Berkeley National Laboratory, Berkeley, California 94720, USA

and replace those contributions with a simpler, long-range dispersion correction based on intermolecular perturbation theory. Here, we demonstrate that one can avoid calculating the long-range MP2 correlation by attenuating the Coulomb operator, allowing the dispersion correction to handle the long-range interactions inexpensively. With relatively modest Coulomb attenuation, one obtains results that are very similar to those from conventional MP2C. With more aggressive attenuation, one can remove just enough short-range repulsive exchange-dispersion interactions to compensate for finite basis set errors. Doing so makes it possible to approach complete-basis-set-limit quality results with only an aug-cc-pVTZ basis, resulting in substantial computational savings. Further computational savings could be achieved by reformulating the MP2C algorithm to exploit the increased sparsity of the two-electron integrals.

Graphical TOC Entry

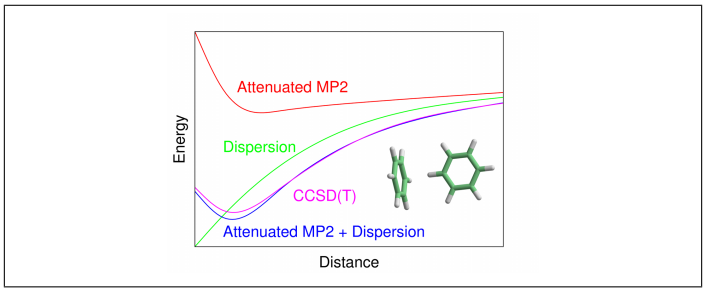

1 Introduction

Non-covalent interactions play a critical role in biological systems, liquids, molecular crystals, and many other systems. In recent years, considerable effort has been devoted to developing electronic structure methods capable of treating the full spectrum of intermolecular interactions with high accuracy. This means developing approximate methods capable of describing interactions such as hydrogen bonding, electrostatics, polarization, and van der Waals dispersion for different intermolecular orientations and separations.

Density functional theory (DFT) and second-order Møller-Plesset perturbation theory (MP2) are both widely used for modeling such interactions.[1] Widely-used semi-local density functionals do not properly describe van der Waals dispersion interactions,[2] but a variety of improved functionals and dispersion corrections have been developed in recent years.[3–9] Alternatively, MP2 is the simplest of the standard wavefunction-based approximations that is capable of describing dispersion and other interactions, and algorithm developments have made it much more computationally affordable.[10–14] Unfortunately, MP2 dramatically overestimates dispersion interactions in π-stacked systems like the benzene dimer and many other cases.[1,15] DFT-based symmetry-adapted perturbation theory (SAPT(DFT)) offers a third alternative, providing good-quality interaction energies at reasonable computational cost.[16–18]

The poor performance of MP2 for dispersion interactions arises from the fact that it describes the intermolecular dispersion at the uncoupled Hartree-Fock (UCHF) level.[19,20] Therefore, a number of researchers have proposed various dispersion corrections based on subtracting out the UCHF dispersion in MP2 and replacing it with a more accurate dispersion model.[21–24] The MP2C model,[22,23] which replaces the UCHF dispersion with a SAPT(DFT) coupled Kohn-Sham (CKS) treatment of intermolecular dispersion has proved particularly effective.[1,23,25–31] It achieves accuracy approaching CCSD(T) across a broad region of the potential energy surface with only $O(N^5)$ computational cost.

The evaluation of the dispersion correction is non-trivial, but two of us recently demonstrated that the dispersion correction can be evaluated in a monomer-centered (MC) basis instead of a

dimer-centered (DC) one with little loss in accuracy.[31] For a single dimer interaction energy calculation, this simple change reduces the computational time by a factor of up to ∼8. On the other hand, if one is evaluating many different points on the potential energy surface, as in a fragment-based molecular crystal calculation, one can achieve ∼100-fold speed-ups in the dispersion correction.

However, MC-basis MP2C is in some sense computationally absurd: When computing the lattice energy of crystalline aspirin using a fragment-based approach, for instance, 99.9% of the time is spent performing the RI-MP2 calculation (including Hartree-Fock), while the remaining 0.1% of the time is spent on the MP2C dispersion correction.[31] A sizable fraction of the MP2 calculation is spent computing the long-range dispersion interactions at the MP2 level, only to discard those contributions and replace them with an inexpensive $O(N^4)$ CKS dispersion energy. Could we simply avoid computing those long-range MP2 correlation effects in the first place, and thereby drastically reduce the necessary computational effort?

Coulomb attenuation/range separation provide an effective means for separating short- and long-range Coulomb interactions, which has been used to increase algorithmic efficiency or develop physically improved density functionals, for instance.[32–59] In this paper, we utilize Coulomb attenuation to eliminate long-range correlation at the MP2 level.[56,57,60,61] Then, we apply a modified MP2C dispersion correction which removes any residual UCHF dispersion remaining in the attenuated MP2 model and adds a long-range CKS dispersion energy to account for the long-range electron correlation. This model enables aggressive Coulomb attenuation at the MP2 level, which allows for both substantial computational savings and higher accuracy than that provided by conventional, finite-basis MP2C. Specifically, benchmark tests indicate that attenuation reduces the MP2C/aug-cc-pVTZ errors roughly in half and gives results approaching complete-basis-set (CBS) quality at drastically lower cost. We also provide new physical insights into how attenuated MP2 approximations are able to achieve these good results.

2 Theory

The MP2C correction works by replacing the UCHF treatment of dispersion found in MP2 with an improved one calculated at the CKS level.

$$E_{MP2C} = E_{MP2} - E_{disp}^{UCHF} + E_{disp}^{CKS} \tag{1}$$

One can understand this qualitatively in terms of the dispersion interaction term from second-order intermolecular perturbation theory,[62]

$$E_{disp} = \sum_{m,n\neq 0} \frac{|\langle \phi_0^A \phi_0^B | \hat{V}^{AB} | \phi_m^A \phi_n^B \rangle|^2}{E_m^A - E_0^A + E_n^B - E_0^B} \tag{2}$$

where ϕ_0 represents the ground state wavefunction for isolated molecules A or B with energy E_0, ϕ_n represents the n-th excited state with energy E_n, and $\hat{V}^{AB}$ is the interaction operator between the molecules (the perturbation). In MP2 or UCHF, these contributions are effectively evaluated using a Koopmans' theorem-style approximation. That is, one neglects any orbital relaxation due to promoting an electron from an occupied to virtual orbital, and one assumes the excitation energy is simply the unrelaxed orbital energy difference. In MP2C, one replaces this simplistic approximation for the excited states and excitation energies with an improved description computed using time-dependent density functional theory (a.k.a. CKS theory). Here, we seek to combine this idea with attenuated MP2.

In the attenuated MP2 approach of Goldey and Head-Gordon,[56,57] one range-separates the Coulomb operator according to

$$\frac{1}{r} = \frac{\mathrm{terf}(r;r_0)}{r} + \frac{\mathrm{terfc}(r;r_0)}{r} \tag{3}$$

where[63]

$$\mathrm{terf}(r;r_0) = \frac{1}{2}\left\{ \mathrm{erf}\left[\frac{r-r_0}{\sqrt{2}r_0}\right] + \mathrm{erf}\left[\frac{r+r_0}{\sqrt{2}r_0}\right] \right\} \tag{4}$$

and

$$\mathrm{terfc}(r;r_0) = 1 - \mathrm{terf}(r;r_0). \tag{5}$$

The function $\mathrm{terfc}(r;r_0)/r$ describes the short-range Coulomb interaction, while $\mathrm{terf}(r;r_0)/r$ describes the long-range contribution. The user-defined parameter r_0 controls the relative length-scales of the two components, with smaller values of r_0 corresponding to a more rapid decay of the short-range $\mathrm{terfc}(r;r_0)/r$ term. While many different possible forms of the attenuation function are possible, the $\mathrm{terfc}(r;r_0)/r$ form maintains the correct curvature of the Coulomb operator at short-range.[63] This helps ensure that the short-range correlation is minimally affected by the elimination of the long-range correlation.

In attenuated MP2, one discards the long-range correlation by neglecting $\mathrm{terf}(r;r_0)/r$ and replacing the Coulomb operator $1/r$ with $\mathrm{terfc}(r;r_0)/r$ when evaluating the two-electron integrals for the MP2 correlation energy. In the context of a typical resolution-of-the-identity (RI) MP2 implementation (i.e. one that does not fully exploit the sparsity introduced by Coulomb attenuation),[10] this corresponds to constructing the key intermediate B^P_{ia} tensors according to:

$$B^P_{ia} = \sum_Q \left(ia \left| \frac{\mathrm{terfc}(r;r_0)}{r} \right| Q \right) \left(Q \left| \frac{\mathrm{terfc}(r;r_0)}{r} \right| P \right)^{-1/2} \tag{6}$$

In other words, the attenuated Coulomb operator is employed both as the density-fitting metric and for the Coulomb interaction between the pair of electrons. The MP2 correlation energy is then computed as usual by taking products of such B tensors and dividing by the appropriate energy denominator.

Attenuating MP2 removes some, but not all, of the intermolecular dispersion from MP2. Therefore, when restoring the long-range dispersion at the CKS level, one must take care to avoid double-counting the intermediate-range dispersion contributions. Accordingly, in attenuated MP2C, we subtract out whatever residual dispersion remains in attenuated MP2 by computing the UCHF contribution using the same attenuated Coulomb operator, and then we add the full CKS dispersion

(without any attenuation):

$$E_{MP2C}(atten.) = E_{MP2}(atten.) - E_{disp}^{UCHF}(atten.) + E_{disp}^{CKS}(full) \tag{7}$$

Because algorithms for conventional MP2C have been published previously,[23,31] we focus only on the necessary modifications to the UCHF term here. No changes are needed in the evaluation of the CKS dispersion energy.

For consistency with the underlying attenuated MP2, attenuation is applied both in the density fitting and the Coulomb interaction components in the UCHF dispersion. This means that one replaces the standard $1/r$ Coulomb operator with $\mathrm{terfc}(r;r_0)/r$ when computing the UCHF monomer frequency-dependent density-density response functions,

$$[\chi_0(\omega)]_{PQ} = -4\sum_{ia} \frac{(P|\mathrm{terfc}(r;r_0)/r|ia)\varepsilon_{ia}(ia|\mathrm{terfc}(r;r_0)/r|Q)}{\varepsilon_{ia}^2 + \omega^2} \tag{8}$$

where i and a are occupied and virtual molecular orbitals, and P and Q are auxiliary basis functions. The quantity $\varepsilon_{ia} = \varepsilon_a - \varepsilon_i$ is the difference between the Hartree-Fock orbital energies for orbitals i and a. One makes the same substitution when transforming this response function using the density-fitting Coulomb metric $S = (P|\mathrm{terfc}(r;r_0)/r|Q)$,

$$\tilde{\chi}_0(\omega) = \mathbf{S}^{-1}\chi_0(\omega)\mathbf{S}^{-1} \tag{9}$$

and in the intermolecular Coulomb integrals $J^{AB} = (P|\mathrm{terfc}(r;r_0)/r|Q)$ that arise in the final Casimir-Polder integration:

$$E_{disp}^{UCHF} = -\frac{1}{2\pi}\int_0^\infty d\omega \tilde{\chi}_0^A(\omega)\mathbf{J}^{AB}(\tilde{\chi}_0^B(\omega))^T(\mathbf{J}^{AB})^T \tag{10}$$

For the J^{AB} integrals, auxiliary basis function P resides on molecule A while auxiliary basis function Q resides on molecule B. Note that all of the necessary MP2C integrals can be performed using either a dimer-centered[23] or monomer-centered basis.[31]

The final step requires choosing the parameter r_0 to determine how aggressively the Coulomb

operator will be attenuated. In the limit as $r_0 \to 0$, $\mathrm{terfc}(r;r_0)/r \to 0$, and one attenuates the MP2C correlation energy completely, leaving only the Hartree-Fock energy plus CKS dispersion. In the limit where $r_0 \to \infty$, $\mathrm{terfc}(r;r_0)/r \to 1/r$, restoring the full Coulomb operator and conventional MP2C. In practice, the parameter r_0 is chosen empirically, as described in Section 4.

The purpose of this paper is evaluate the physical behavior and accuracy of attenuated MP2C. Substantial computational savings are achieved through the cancellation of finite-basis-set errors via Coulomb attenuation, which allows one to obtain large-basis-quality results with much smaller basis sets. Additional savings ought be achievable by reformulating the MP2C algorithm to exploit the short-range nature of the modified Coulomb operator, but such a reformulation has not yet been accomplished.

3 Computational Methods

Attenuated MP2 and MP2C have been implemented in a development version of Q-Chem.[64] Most MP2 calculations performed here utilized the dual-basis Hartree-Fock[12] and resolution-of-the-identity (RI) MP2 approximations,[10,65,66] along with the corresponding Dunning aug-cc-pVTZ or aug-cc-pVQZ basis sets.[67–69] Only valence electrons were correlated.

The MP2C dispersion correction calculations were performed using either Q-Chem or Molpro.[70] For the CKS calculations in Q-Chem, the local Hartree-Fock orbitals were obtained from Molpro and read into Q-Chem. Counterpoise (CP) corrections for basis set superposition error (BSSE) were performed in all cases unless otherwise specified. Extrapolations to the complete basis set limit were performed separately for the HF and correlation energies using two-point formulas.[71,72]

This work focuses on attenuated MP2C in the aug-cc-pVTZ basis. The aug-cc-pVTZ basis provides significant improvements over aug-cc-pVDZ at the attenuated MP2 level,[57] and it is sufficiently large to provide fairly well-converged MP2C dispersion corrections.[23,31]

Finally, the key calculated interaction energies used to produce the figures and tables presented

below are provided as supporting information.

4 Results and Discussion

4.1 Understanding attenuated MP2

Before discussing attenuated MP2C, we first examine how attenuated MP2 behaves on the S66 dimer interaction test set.[73] To do so, we decompose the attenuated MP2 errors relative to the estimated CBS-limit CCSD(T) benchmarks,[73] $E(attMP2/aTZ) - E(CCSD(T)/CBS,CP)$ into contributions arising from the finite basis set, the post-MP2 correlation error, and the error introduced by attenuating the Coulomb operator. For attenuated MP2/aug-cc-pVTZ without CP-correction, for instance, these errors are defined as:

$$\text{Finite-basis error:} \quad E(MP2/aTZ,no\text{-}CP) - E(MP2/CBS,CP) \tag{11}$$

$$\text{Correlation error:} \quad E(MP2/CBS,CP) - E(CCSD(T)/CBS,CP) \tag{12}$$

$$\text{Attenuation error:} \quad E(attMP2/aTZ,no\text{-}CP) - E(MP2/aTZ,no\text{-}CP) \tag{13}$$

The total error is the sum of the these three contributions. Counterpoise-corrected attenuated MP2/aug-cc-pVTZ can be partitioned analogously, except the counterpoise correction is applied to all terms in the expressions above.

For attenuated MP2/aug-cc-pVTZ without counterpoise correction (Figure 1a), basis set superposition error leads to overbinding of the dimer. The inadequate treatment of electron correlation in MP2 also frequently leads to overbinding the dimers, particularly for the dimers where dispersion interactions are important. Figure 1a shows that these errors range from a few kJ/mol up to nearly 10 kJ/mol in π-stacking cases like benzene dimer. Together, these two error sources lead to systematic overbinding of the dimers. On the other hand, applying Coulomb attenuation reduces the long-range intermolecular correlation (i.e. attractive long-range dispersion interactions) and weakens the binding. Attenuated MP2 works, therefore, by choosing an appropriate value of

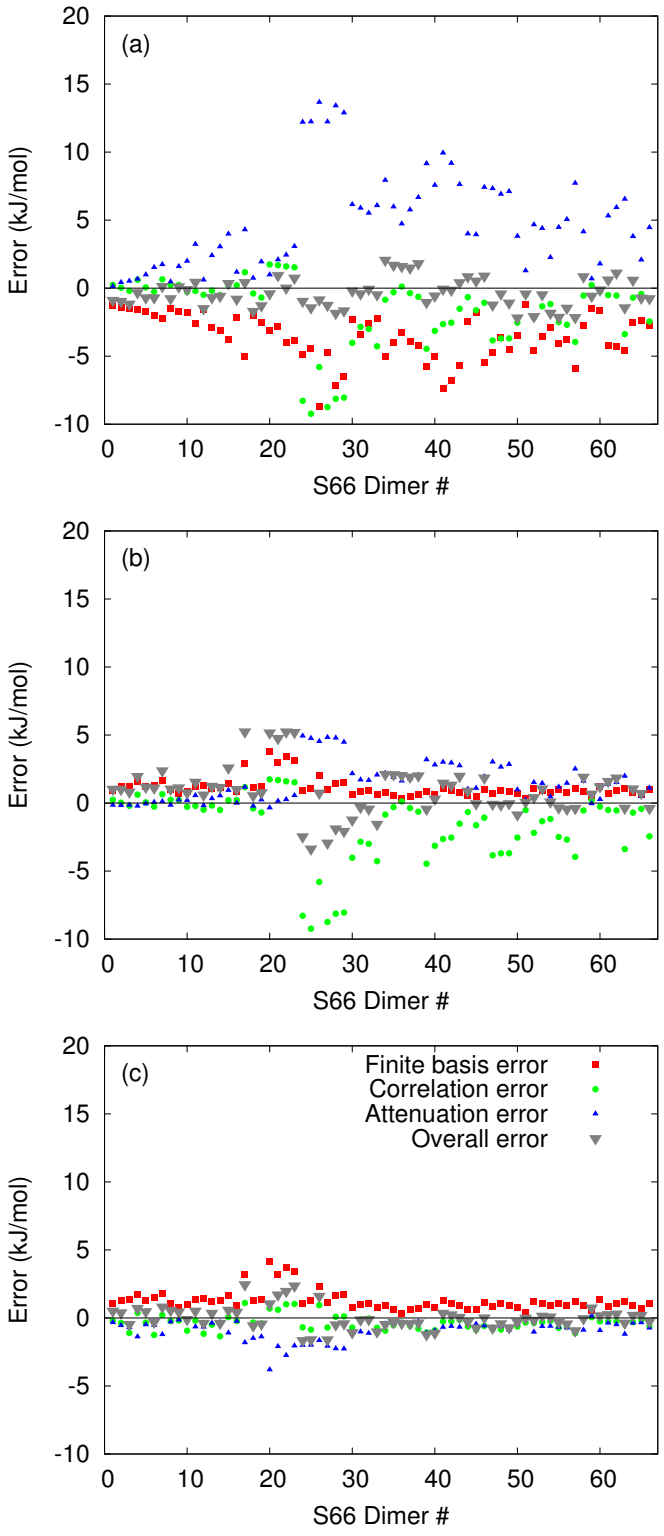

Figure 1: Error contributions for each dimer in the S66 set and aug-cc-pVTZ basis set for (a) attenuated MP2 without counterpoise correction ($r_0 = 1.35$ Å), (b) attenuated MP2 with counterpoise correction ($r_0 = 1.75$ Å), and (c) attenuated MP2C with counterpoise correction ($r_0 = 0.9$ Å). The energy-decomposition of the errors is described in the main text.

r_0 (e.g. $r_0 = 1.35$ Å for the aug-cc-pVTZ basis[57]) such that one attenuates enough of the long-range correlation to cancel out the large errors arising from the finite basis set and the MP2-level treatment of correlation.

Applying a counterpoise correction to attenuated MP2 greatly reduces the basis set error, as shown in Figure 1b. It also changes the sign of the basis set error: counterpoise-corrected aug-cc-pVTZ interaction energies are generally underbound, unlike their non-counterpoise-corrected counterparts. However, MP2 correlation still often overestimates the interaction energies, and the sum of the basis set and correlation errors leads to overbinding for many of the S66 dimers. Once again, one can choose an appropriate degree of Coulomb attenuation to reduce this overbinding. Because the errors that need to be cancelled in this case are generally smaller, one attenuates less aggressively to keep a larger fraction of the long-range correlation. Hence, the optimal r_0 value for counterpoise-corrected MP2/aug-cc-pVTZ is 1.75 Å instead of 1.35 Å for the non-counterpoise-corrected case.[57] There are notable cases like the acetamide dimer, however, where the combined basis set and MP2 correlation errors lead to underbinding when a counterpoise correction is employed. In such cases, attenuating the long-range attractions actually increases the errors. This explains the earlier finding that attenuated-MP2 actually performs better without a counterpoise correction for the S66 test set.[57]

To summarize, attenuated MP2 works for intermolecular interactions by cancelling several different sources of error with opposite signs: One attenuates away enough of the attractive dispersion interaction from MP2 to cancel the overbinding of intermolecular interactions that typically occurs with MP2 in finite basis sets. Because attenuated MP2 relies on the cancellation of large individual error terms, it can be very sensitive to the choice of r_0, as seen previously.[56,57]

4.2 Attenuated MP2C and the optimal r_0 parameter value

Next we consider attenuated MP2C. A similar energy decomposition can be performed for counterpoise-corrected MP2C in the aug-cc-pVTZ basis,

$$\text{Finite-basis error:} \quad E(MP2C/aTZ,CP) - E(MP2C/CBS,CP) \tag{14}$$

$$\text{Correlation error:} \quad E(MP2C/CBS,CP) - E(CCSD(T)/CBS,CP) \tag{15}$$

$$\text{Attenuation error:} \quad E(attMP2C/aTZ,CP) - E(MP2C/aTZ,CP) \tag{16}$$

as shown in Figure 1c. The MP2C dispersion correction is already fairly well converged in the aug-cc-pVTZ basis,[31] so the basis set error here is nearly identical to the basis set error for counterpoise-corrected attenuated MP2 (Figure 1b). However, the dispersion correction dramatically reduces the correlation error. The MP2C correlation error has no systematic bias and is typically smaller than the basis set error. Because the basis set error dominates, the sum of these two contributions leads to systematic underbinding of the dimers, which is the opposite of the overbinding seen in the MP2 case.

Table 1: Root-mean-square errors for the S66 test set relative to CCSD(T)/CBS with optimal r_0 values.

Method	Basis	BSSE	Optimal r_0 (Å)	RMS Error (kJ/mol)
MP2	aug-cc-pVTZ	no CP	—	6.4
MP2	aug-cc-pVTZ	CP	—	2.9
atten. MP2	aug-cc-pVTZ	CP	1.75	2.0
atten. MP2	aug-cc-pVTZ	no CP	1.35	1.1
MP2	CBS-limit	CP	—	3.1
MP2C	aug-cc-pVTZ	no CP	—	4.1
MP2C	aug-cc-pVTZ	CP	—	1.5
atten. MP2C	aug-cc-pVTZ	CP	0.9	0.8
MP2C	CBS-limit	CP	—	0.6

We now seek an appropriate attenuation parameter r_0 to compensate for these errors in MP2C. Figure 2 plots rms errors for the S66 test set (the same set was used to parameterize attenuated

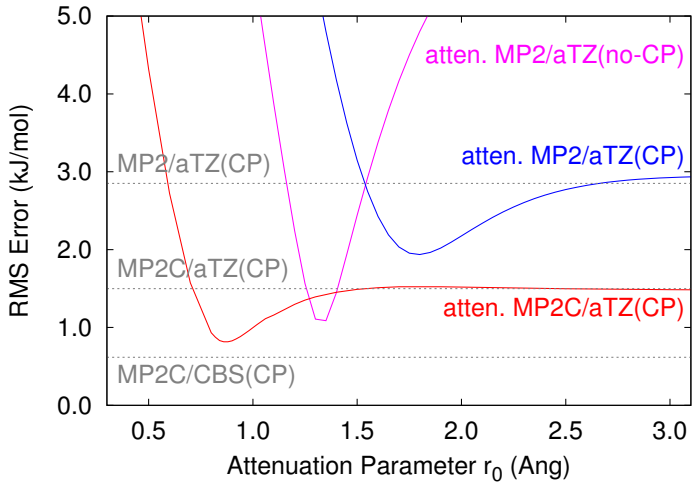

Figure 2: Root-mean-square errors (in kJ/mol) for attenuated MP2,[57] attenuated MP2C, standard MP2, and standard MP2C relative to the CCSD(T) benchmarks for the S66 test set. Compared to attenuated MP2, attenuated MP2C achieves higher accuracy, is less sensitive to the value of r_0, and allows for more aggressive attenuation (a smaller r_0 value). Note that attenuated MP2 error does asymptote to the conventional MP2 result for large r_0 values beyond the range plotted here.

MP2) as a function of r_0. For values of $r_0 > 1.5$ Å, attenuated MP2C results are very close to their unattenuated counterparts. Decreasing r_0 further reduces the rms errors until a minimum is reached around $r_0 = 0.9$ Å, with an rms error of only 0.8 kJ/mol. For r_0 values smaller than 0.9 Å, the rms errors increase once again.

The 0.8 kJ/mol rms error for attenuated MP2C/aug-cc-pVTZ at the optimal r_0 value is roughly half the error of conventional MP2C in the same basis, and it approaches the 0.6 kJ/mol accuracy of CBS-limit MP2C. The attenuated MP2C accuracy is somewhat higher than the smallest errors achieved by attenuated MP2 (see Figure 2 and Table 1). Moreover, the attenuated MP2C results are much less sensitive to the choice of the r_0 parameter than attenuated MP2.

Attenuated MP2C also allows for more aggressive Coulomb attenuation than attenuated MP2 ($r_0 = 0.9$ Å versus $r_0 = 1.35$ Å), which should lead to additional computational savings in an efficient implementation that exploits the sparsity of the two-electron integrals. As shown in Figure 3, the attenuated Coulomb operator dies off completely within 7–8 Å when $r_0 = 0.9$ Å, which will significantly increase the sparsity of the electron repulsion integrals compared to using larger r_0 values or the conventional Coulomb operator. Generally speaking, the number of electron repulsion

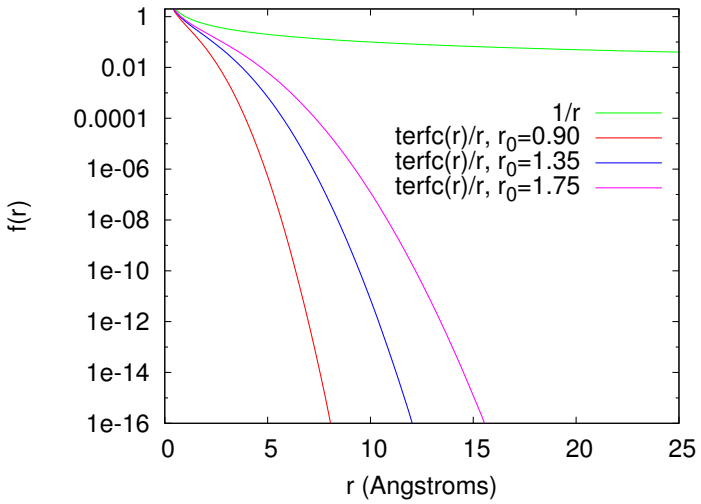

Figure 3: Attenuation with any of the optimal r_0 values in Table 1 dramatically reduces the range of the Coulomb operator, but the more aggressive attenuation ($r_0 = 0.9$ Å) possible for attenuated MP2C leads to a modified Coulomb operator that dies off completely by 7–8 Å.

integrals grows quartically with system size. Accounting for overlap sparsity reduces that growth to quadratic, while attenuation of the sort used here will reduce that growth to linear over rather short length scales. Some numerical investigations of this behavior have been reported previously using a slightly different $(\mathrm{erfc}(\omega r)/r)$ form of Coulomb attenuation.[74]

Returning to Figure 1c, we observe that the error introduced by attenuating MP2C with $r_0 = 0.9$ Å does indeed largely cancel the finite-basis and correlation errors to produce the overall high accuracy. However, the sign of the MP2C attenuation error is opposite to that of the MP2 attenuation error, indicating that different physics are involved.

To understand this difference, Figure 4 plots the rms energy change between the attenuated and non-attenuated versions of MP2, MP2C, and the UCHF dispersion component for the S66 set as a function of the attenuation parameter. The changes in the attenuated UCHF dispersion energies overlap with the changes in the attenuated MP2 results almost perfectly. In other words, for intermolecular interactions, attenuating medium- and long-range MP2 correlation is essentially equivalent to attenuating the UCHF dispersion. Only at shorter r_0 values, where exchange-dispersion effects become important, do the attenuated UCHF dispersion and attenuated MP2 curves diverge. Note that contributions like intermolecular polarization are handled at the HF level.

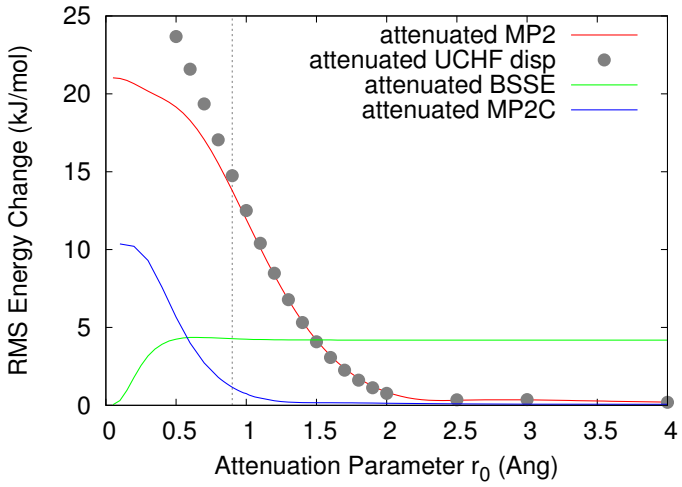

Figure 4: Root-mean-square energy change between the attenuated and unattenuated MP2, UCHF dispersion, and MP2C models in the aug-cc-pVTZ basis. The rms change in the MP2/aug-cc-pVTZ counterpoise correction due to attenuation is also shown ("attenuated BSSE"). The dashed vertical line indicates $r_0 = 0.9$ Å.

Subtracting the UCHF dispersion energy from the MP2 energy in MP2C, $E_{MP2} - E_{disp}^{UCHF}$, produces an intermolecular "dispersion-free" MP2 model, to which the CKS dispersion subsequently added. With the intermolecular UCHF dispersion removed, the intermolecular interactions are nearly independent of the attenuation parameter for $r_0 > 1.5$ Å, as indicated by the attenuated MP2C curve in Figure 4 (because the CKS dispersion contribution is not attenuated, it cancels when taking the difference between the attenuated and standard models in Figure 4). In other words, Coulomb attenuation eliminates interactions that are discarded anyways when computing the MP2C dispersion correction, which explains why attenuated MP2C gives virtually identical results to conventional MP2C for $r_0 > 1.5$ Å in Figure 2.

If one chooses to attenuate more aggressively using r_0 values below 1.5 Å, however, short-range exchange-dispersion energy begins to be attenuated, as indicated by the rapid increase in the MP2C energy change for small r_0 (Figure 4). Unlike dispersion energies, exchange-dispersion interactions are repulsive, and attenuating them increases the strength of the intermolecular binding. This allows one to compensate for the finite-basis errors in MP2C/aug-cc-pVTZ and achieve near CBS-limit accuracy (Figure 2). It explains why the MP2C attenuation error has the opposite sign

of the MP2 attenuation error in Figure 1, and this difference in sign is exactly what is needed to cancel the basis set error.

It is also important to recognize that one must use a counterpoise correction to obtain accurate results with attenuated MP2C. As shown in Figure 4, Coulomb attenuation does not significantly reduce the BSSE (as measured by the size of the counterpoise correction) until $r_0 < 0.5$ Å, which is well-below the r_0 range for which accurate attenuated MP2 or MP2C results are obtained. If one omits the counterpoise correction, the combined basis set and correlation errors cause overbinding. One cannot compensate for this overbinding by attenuating the repulsive exchange-dispersion interaction—attenuating MP2C only binds the dimers more strongly. On the one hand, the need for a counterpoise correction does make attenuated MP2C more expensive than attenuated MP2, for which the counterpoise correction is neither necessary nor desirable. On the other hand, the magnitudes of the error cancellations involved in attenuated MP2C are much smaller, which reduces its sensitivity to the value of the parameter r_0 and makes the model more transferable to other systems, as demonstrated below.

4.3 Transferability of attenuated MP2C

To be useful, attenuated MP2 and MP2C should perform well for systems other than those against which the attenuation parameter r_0 was optimized. This section examines the transferability of attenuated MP2 and MP2C using the optimal r_0 values reported in Table 1. Dimer-centered basis sets were used unless otherwise specified.

First we consider the S22x5 test set,[25] which consists of 22 different dimers than the S66 test set at five different intermolecular spacings each. Here, it tests both the transferability of the different approximations across different species and away from equilibrium separations. Figure 5 plots the errors relative to the CCSD(T) benchmark values for various different methods. At equilibrium separation ($1.0R_e$), the conventional MP2 errors here are nearly twice as large as they were for the S66 set. Similarly, the attenuated MP2 errors are also twice as large, though they still represent a significant improvement over conventional MP2/CBS. Attenuated MP2 performs worse away from

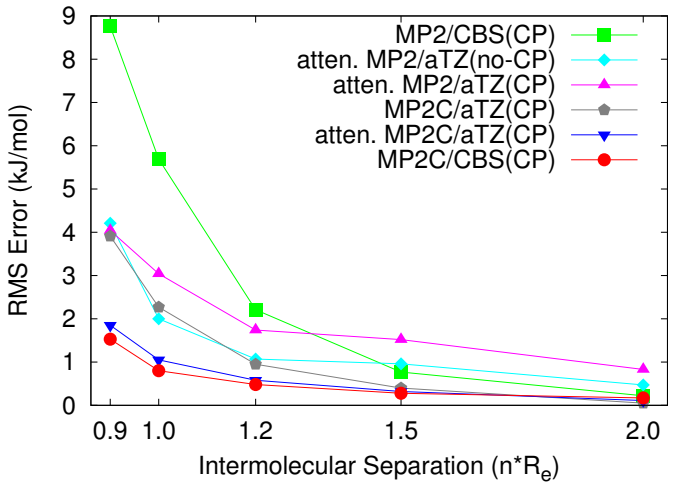

Figure 5: Performance of attenuated MP2 and MP2C on the S22x5 test set relative to the CCSD(T) benchmark values. The errors for attenuated MP2 are much larger here, particular at shorter distances, while attenuated MP2C/aug-cc-pVTZ gives results that are very close to the MP2/CBS values.

the equilibrium separation, however. The errors rise rapidly at $0.9R_e$, and they do not head toward zero as rapidly as expected toward longer separations.

Attenuated MP2C performs much better on the S22x5 set. The MP2C/CBS error at $1.0R_e$ is only about 25% worse than it was for the S66 set, and attenuated MP2C mimics this behavior. More importantly, attenuated MP2C tracks the CBS-limit MP2C results very closely across the entire potential energy surface. This represents a substantial improvement over conventional MP2C in the aug-cc-pVTZ basis. These results reflect both how MP2C provides a better starting point than MP2, and how having smaller errors to cancel and a reduced dependence on the parameter r_0 improves the transferability of attenuated MP2C relative to attenuated MP2.

Second, we consider the 1HSG test set,[75] which is comprised of 21 sets of fragment interactions extracted from the active site of a protein-ligand complex and which is chemically very different from the S66 and S22x5 sets, making it another good test for transferability. In this case, conventional MP2/aug-cc-pVTZ exhibits an rms error of 1.2 kJ/mol relative to the CCSD(T) benchmarks (Table 2). Extrapolating to the CBS-limit reduces the MP2 errors to 0.9 kJ/mol. MP2C provides noticeable improvements over MP2, with rms errors of 1.0 and 0.5 kJ/mol in the aug-cc-pVTZ

Table 2: Root-mean-square errors relative to benchmark CCSD(T) values for the interaction energies in the 1HSG test set. MC and DC basis refer to the basis used to compute the MP2C dispersion correction, if appropriate.

Method	Basis	BSSE	RMS Error	
			DC basis	MC basis
MP2	aug-cc-pVTZ	no CP	3.6	
MP2	aug-cc-pVTZ	CP	1.2	
atten. MP2 ($r_0 = 1.75$ Å)	aug-cc-pVTZ	CP	1.9	
atten. MP2 ($r_0 = 1.35$ Å)	aug-cc-pVTZ	no CP	0.9	
MP2	CBS-limit	CP	0.9	
MP2C	aug-cc-pVTZ	CP	1.0	1.1
atten. MP2C [a]	aug-cc-pVTZ	CP	0.5	0.5
MP2C	CBS-limit	CP	0.5	0.5

[a] $r_0 = 0.9$ Å for the DC basis and $r_0 = 0.82$ Å for the MC basis.

basis and CBS-limit, respectively.

Attenuated MP2 without a counterpoise correction performs reasonably well, with an rms error of 0.9 kJ/mol, comparable to the CBS-limit MP2 or aug-cc-pVTZ basis MP2C results. The counterpoise-corrected version of attenuated MP2, however, cannot be recommended, since it doubles the errors relative to the version without counterpoise correction. Both cases contrast the results from the S66 test set, where attenuated MP2 out-performs CBS-limit MP2 by a wide margin. On the other hand, attenuated MP2C once again performs on par with CBS-limit MP2C, with an 0.5 kJ/mol rms error that is half that of the errors obtained with conventional MP2C/aug-cc-pVTZ or attenuated MP2. These results further demonstrate the transferability of the optimal attenuation parameter r_0 for MP2C.

One should recognize, however, that the nature of the error cancellation in attenuated MP2C is approximate, and that the optimal value of r_0 was chosen in Section 4.2 to minimize errors with respect to the CCSD(T) benchmarks. Therefore, although the MP2C/CBS and attenuated MP2C/aug-cc-pVTZ errors are statistically competitive in the 1HSG test set, the two methods do not necessarily predict identical interaction energies for individual dimers. Coulomb attenuation overcompensates for finite-basis errors in some dimers, while under-correcting it in others, as shown in Figure 6. Similar conclusions hold for the other data sets examined here.

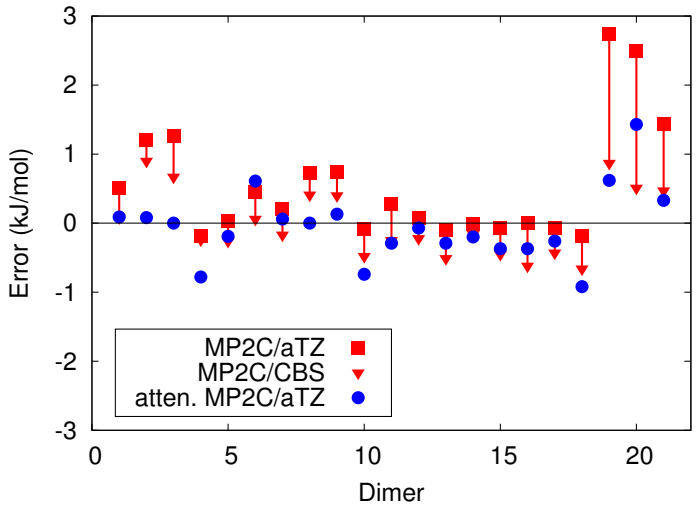

Figure 6: Errors for individual dimers in the 1HSG test set. The arrows indicate the effect of improving the basis in conventional MP2C. Attenuated MP2C sometimes underestimates the finite-basis error and sometimes overestimates it. Overall, however, it produces results that are statistically comparable to conventional CBS-limit MP2C.

Finally, we apply attenuated MP2C to determine the lattice energies for several small-molecule crystals benchmarked previously using the fragment-based hybrid many-body interaction (HMBI) approach (Figure 7).[31,76,77] Specifically, attenuated MP2C was used to evaluate the interaction energies between pairs of molecules (2-body terms) in the fragment approach. Conventional, unattenuated MP2/aug-cc-pVTZ was used for the intramolecular (1-body) contributions for the reasons discussed in Section 4.5.

Earlier work has demonstrated that conventional MP2 in large basis sets predicts lattice energies within a few kJ/mol of benchmark CCSD(T) results for crystals where dispersion is not important. In crystals such as benzene or imidazole where dispersion interactions play a significant role, however, MP2 overestimates the lattice energy by 10–15 kJ/mol ($\sim$15–20%).[76,77] For the seven crystals considered here, CBS-limit MP2 exhibits a root-mean-square error of 6.8 kJ/mol relative to CCSD(T). CBS-limit MP2C performs somewhat better for the lattice energies of these crystals, with an rms error of 2.3 kJ/mol relative to the CCSD(T) values.[31]

Due to finite-basis limitations, MP2C/aug-cc-pVTZ lattice energies are slightly worse than the CBS values, as shown in Figure 7, with an rms error of 4.5 kJ/mol. Attenuated MP2C/aug-cc-

pVTZ increases the lattice energies in the direction of the CBS limit, binding the crystals more tightly. In some cases, the attenuation correction undershoots MP2C/CBS (e.g. ice, ammonia, and carbon dioxide), while in others it overshoots (e.g. imidazole and benzene). Nevertheless, attenuated MP2C/aug-cc-pVTZ gives a root-mean-square error of only 3.7 kJ/mol, which is a modest improvement over conventional MP2C/aug-cc-pVTZ (4.5 kJ/mol), but not as accurate as MP2C/CBS (2.3 kJ/mol). Note that the magnitude of the errors in the crystal lattice energies are larger than those for the S66, S22x5, and 1HSG test sets discussed earlier because they result from summing over hundreds of dimer interactions when calculating the crystal lattice energies.

The two most notable errors occur in carbon dioxide and imidazole. In carbon dioxide, the difference between attenuated MP2C/aug-cc-pVTZ and CBS-limit MP2C arises almost entirely from the 1-body intramolecular contributions, for which conventional MP2/aug-cc-pVTZ was used. The two-body contributions computed with attenuated MP2C match the CBS-limit MP2C values very well. For imidazole, MP2C itself overestimates the lattice energy,[31] and attenuated MP2C mimics this behavior. Interestingly, attenuated MP2/aug-cc-pVTZ (no CP correction) performs about as well as attenuated MP2C on these crystals, with a root-mean-square error of 3.9 kJ/mol. While it performs somewhat worse for formamide, acetamide, and benzene, attenuated MP2 performs better than MP2C for imidazole (Figure 7).

In the future, it would be interesting to examine to what extent this attenuation properly preserves the appropriate energetic ordering of different crystal packing motifs, which can be very sensitive to the electronic structure treatment.[78–84]

In summary, the Coulomb attenuation parameter r_0 obtained for MP2C/aug-cc-pVTZ in Section 4.2 appears to be generally transferable across a variety of benchmark systems. In all cases, the results obtained with attenuated MP2C/aug-cc-pVTZ are statistically approaching the quality of those predicted by conventional MP2C/CBS, but they can be evaluated with much lower computational cost.

Even though the current implementation of attenuated MP2C does not exploit the increased integral sparsity, it still achieves substantial speed-ups by avoiding the need for larger basis sets.

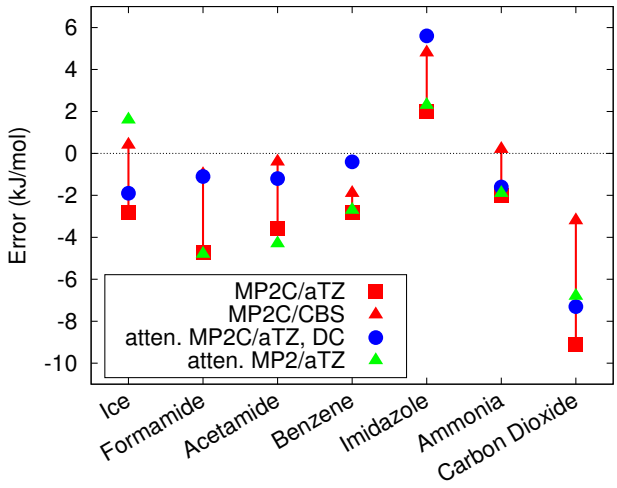

Figure 7: Errors in lattice energy predictions relative to estimated CBS-limit CCSD(T) benchmarks.[76,77] For the attenuated MP2C results, attenuation was applied only to the intermolecular (two-body) contributions. Conventional MP2/aug-cc-pVTZ was used for the intramolecular (1-body) contributions.

For example, for a conventional two-point TZ/QZ basis set extrapolation to the CBS limit, performing counterpoise-corrected attenuated MP2C interaction energy calculations for the stacked benzene dimer from the S22 test set required about 10 hours (aug-cc-pVTZ) and 43 hours (aug-cc-pVQZ) on a single core of a 2.3 Ghz Intel Xeon E5-2630 processor with 4 GB of RAM. For the attenuated version, one can avoid the aug-cc-pVQZ basis calculation entirely, thereby reducing the computational time by 80%.

4.4 Monomer- vs. dimer-centered basis sets

Using a monomer-centered basis set instead of a dimer-centered one can significantly reduce the computational costs associated with evaluating the MP2C dispersion correction. It is well-known that computing accurate UCHF or CKS dispersion energies requires large basis sets,[85] but for conventional MP2C at least, it turns out that the difference $E_{disp}^{CKS} - E_{disp}^{UCHF}$ is much less sensitive to basis set. For instance, for the S22 test set, the rms difference between MC and DC basis sets for MP2C/aug-cc-pVTZ is only 0.14 kJ/mol.[31]

Because attenuated MP2C attenuates the UCHF dispersion contribution but not the CKS one,

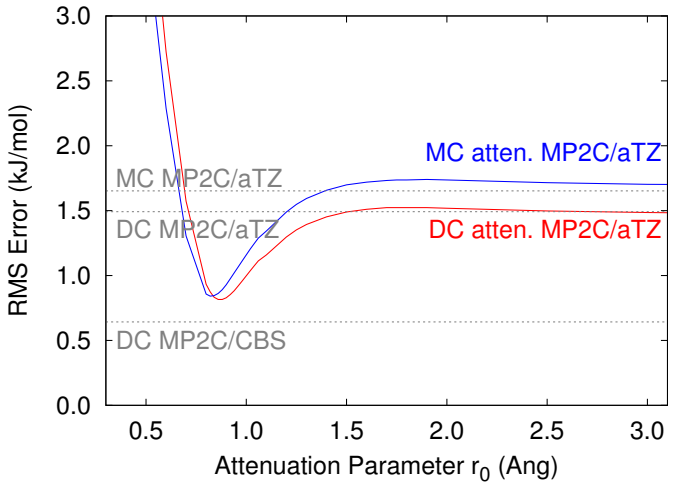

Figure 8: Difference between MC and DC attenuated MP2C/aug-cc-pVTZ for the S66 test set as a function of the attenuation parameter r_0. All results employ a counterpoise correction.

the balance could conceivably be upset. However, as shown in Figure 8, using an MC basis instead of a DC one has only a small effect on the overall results. Switching from a DC to an MC basis increases the S66 rms error for conventional MP2C by only 0.1–0.2 kJ/mol, which is comparable to what is observed for conventional MP2C. The optimal r_0 value for the MC case does shift slightly lower to 0.82 Å, but the difference in rms error is small. Together, these results suggest that one can still use either an MC or DC basis set when computing the dispersion correction in attenuated MP2C.

The MC basis results appear to be transferable to other systems as well. In the 1HSG test set, for instance, the root-mean-square errors in the MC and DC basis attenuated MP2C differ by less than 0.1 kJ/mol, though individual dimer interactions vary by up to ∼0.2 kJ/mol (see Supporting Information). The MC and DC basis sets give very similar root-mean-square errors for the S22x5 test set too, as shown in Table 3. The molecular crystal lattice energies for the seven crystals tested above change by less than 1 kJ/mol upon switching from a DC to an MC basis, and the overall rms error increases by 0.1 kJ/mol (see Supporting Information).

The similarity of the MC and DC basis attenuated MP2C results are not particularly surprising when one considers that attenuation does not significantly affect the MP2 basis set superposition

Table 3: Root-mean-square errors (in kJ/mol) relative to the CCSD(T) benchmarks for the S22x5 test set using attenuated MP2C with either a DC or MC basis in the dispersion correction.

Separation	DC basis[a]	MC basis[b]
0.9 R_0	1.8	1.5
1.0 R_0	1.0	1.0
1.2 R_0	0.6	0.6
1.5 R_0	0.3	0.4
2.0 R_0	0.1	0.1

[a] Using $r_0 = 0.9$ Å. [b] Using $r_0 = 0.82$ Å.

error until $r_0 < 0.5$ Å (Figure 4). In other words, the impact of ghost atom basis functions does not change much between the unattenuated case and the attenuated case in the $r_0 = 0.8$–0.9 Å regime, so attenuation does not upset the CKS and UCHF basis set error cancellation in MP2C.

4.5 Poor performance for intramolecular interactions

The above results demonstrate the excellent performance of attenuated MP2C for intermolecular interactions. However, the MP2C dispersion correction only affects intermolecular dispersion, since it is based on intermolecular perturbation theory. Therefore, it should come as no surprise that attenuated MP2C performs poorly for intramolecular interactions when using the r_0 value for optimized for intermolecular interactions.

Consider the P76 test set,[86] which consists of many different small-peptide conformers whose relative energies are heavily influenced by intramolecular non-covalent interactions. Because the intermolecular MP2C dispersion correction plays no role in these cases, the only difference between attenuated MP2 and attenuated MP2C in these examples is the value of r_0 used in attenuating MP2. Whereas attenuated MP2/aug-cc-pVTZ with $r_0 = 1.35$ Å performs better than conventional MP2/aug-cc-pVTZ (rms errors of 1.7 vs 2.4 kJ/mol),[57] using $r_0 = 0.9$ Å as in attenuated MP2C attenuates too much of the intramolecular correlation and produces a much larger rms error of 6.5 kJ/mol, which is significantly worse than even conventional MP2 (see Figure 9).

A simple, albeit not entirely satisfactory fix for this problem is to use attenuated MP2C only for intermolecular interactions (i.e. the two-body terms in a many-body expansion), and to compute

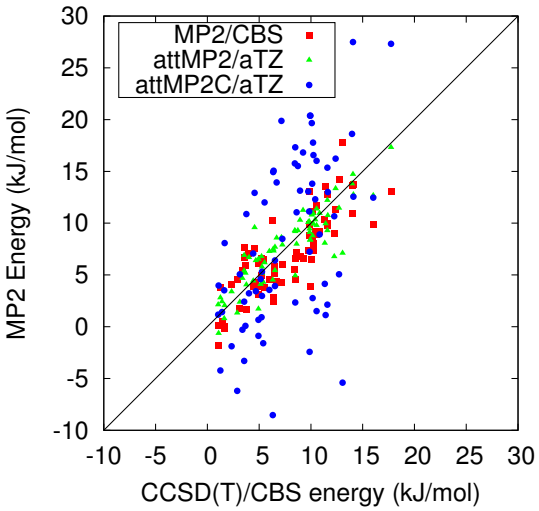

Figure 9: Performance of MP2, attenuated MP2 ($r_0 = 1.35$ Å), and attenuated MP2C ($r_0 = 0.9$ Å) for the P76 test set of peptide conformers in the aug-cc-pVTZ basis. Counterpoise corrections could not applied because they are ill-defined for intramolecular interactions like these.

the intramolecular (one-body) terms with a more appropriate level of theory. For a dimer, for instance, one can compute the total energy as the sum of the energies of each isolated monomer E_A and E_B plus the interaction $\Delta^2 E_{AB}$ between them, $E_{AB} = E_A + E_B + \Delta^2 E_{AB}$. This is the approach used for the molecular crystal benchmarks discussed earlier. One might be able to afford CCSD(T) or use attenuated MP2 for the monomer terms, and then apply attenuated MP2C to compute the interaction energy $\Delta^2 E_{AB}$, for instance.

A better solution might involve correcting the intramolecular dispersion similarly to the intermolecular dispersion using an atom-centered dispersion coefficient representation.[24] Investigation of such an approach is on-going.

5 Conclusions

In this paper, we have extended the idea of Coulomb attenuation of the correlation energy using a double error function to MP2C for the treatment of intermolecular interactions. Several key conclusions regarding Coulomb-attenuated methods have emerged in the process:

1. Attenuated MP2 compensates for intermolecular overbinding that typically arises from the

combination of finite-basis error and missing higher-order correlation effects in MP2 by eliminating an appropriate fraction of the attractive UCHF dispersion. The magnitude of error cancellation involved is fairly large relative to the strengths of the interactions involved.

2. MP2C eliminates the UCHF dispersion and replaces it with more accurate CKS dispersion. One can therefore attenuate away the long- and medium-range Coulomb interactions in MP2 (i.e. $r_0 \sim 1.5$ Å) with only a small impact on the MP2C interaction energies.

3. Counterpoise-corrected MP2C/aug-cc-pVTZ typically underbinds dimers due finite-basis-set error. Aggressive Coulomb attenuation ($r_0 = 0.9$ Å) allows one to approximately compensate for this underbinding by removing some of the repulsive exchange-dispersion. This enables one to approach CBS-limit results using only an aug-cc-pVTZ basis, which has substantially lower computational costs.

4. Attenuating the repulsive exchange-dispersion interactions cannot compensate for the overbinding caused by BSSE. It is necessary, therefore, to employ a counterpoise correction to compensate for BSSE with attenuated MP2C.

5. Because the error cancellations involved are much smaller, attenuated MP2C is less sensitive to the attenuation parameter than attenuated MP2, which makes it more transferable across different systems and regions of the potential energy surface.

6. One can use either a monomer-centered or dimer-centered basis set in attenuated MP2C, with dimer-centered basis sets providing marginally better performance.

7. By construction, attenuated MP2C only works well for intermolecular interactions. More research is needed to extend these ideas to systems where the changes in the intramolecular interactions are important.

Overall, Coulomb-attenuated MP2C rectifies many weaknesses of attenuated MP2 and achieves higher accuracy for intermolecular interactions, making it promising for wider application. It provides dimer interaction energies with kJ/mol accuracy relative CBS-limit CCSD(T) interaction en-

ergies with a modest aug-cc-pVTZ basis and $O(N^5)$ scaling. Furthermore, the dramatically shorter length-scale over which the attenuated Coulomb operator acts suggests that one should to be able achieve substantial additional computational savings by exploiting the new-found sparsity in the MP2 two-electron integrals.

6 Acknowledgments

Funding for this work from the National Science Foundation (CHE-1112568, G.B. and Y.H.), the Department of Energy (DE-AC02-05CH11231, M.G. and M.H.G), and supercomputer time from XSEDE (TG-CHE110064, G.B. and Y.H.) are gratefully acknowledged. We also thank Prof. Pavel Hobza for sharing benchmark data for the S22x5 test set.

Supporting Information Available

Computed interaction and conformational energies for the various test sets considered here are provided as supporting information. This material is available free of charge via the Internet at `http://pubs.acs.org`.

References

(1) Riley, K. E.; Pitonak, M.; Jurecka, P.; Hobza, P. *Chem. Rev.* **2010**, *110*, 5023–63.

(2) Kristyan, S.; Pulay, P. *Chem. Phys. Lett.* **1994**, *229*, 175–180.

(3) Dion, M.; Rydberg, H.; Schröder, E.; Langreth, D. C.; Lundqvist, B. I. *Phys. Rev. Lett.* **2004**, *92*, 246401.

(4) Thonhauser, T.; Cooper, V. R.; Li, S.; Puzder, A.; Hyldgaard, P.; Langreth, D. C. *Phys. Rev. B* **2007**, *76*, 125112.

(5) Tkatchenko, A.; Scheffler, M. *Phys. Rev. Lett.* **2009**, *102*, 073005.

(6) DiStasio, R. A.; von Lilienfeld, O. A.; Tkatchenko, A. *Proc. Nat. Acad. Sci.* **2012**, *109*, 14791–14795.

(7) Grimme, S. *WIRES: Comput. Mol. Sci.* **2011**, *1*, 211–228.

(8) Otero-de-la Roza, A.; Johnson, E. R. *J. Chem. Phys.* **2013**, *138*, 204109.

(9) Vydrov, O. A.; Van Voorhis, T. *J. Chem. Phys.* **2010**, *133*, 244103.

(10) Weigend, F.; Häser, M.; Patzelt, H.; Ahlrichs, R. *Chem. Phys. Lett.* **1998**, *294*, 143–152.

(11) Wolinski, K.; Pulay, P. *J. Chem. Phys.* **2003**, *118*, 9497.

(12) Steele, R. P.; Distasio, R. A.; Shao, Y.; Kong, J.; Head-Gordon, M. *J. Chem. Phys.* **2006**, *125*, 074108.

(13) Werner, H.-J.; Manby, F. R.; Knowles, P. J. *The Journal of Chemical Physics* **2003**, *118*, 8149.

(14) Distasio, R. A.; Jung, Y.; Head-Gordon, M. *J. Chem. Theory Comput.* **2005**, *1*, 862–876.

(15) Sinnokrot, M. O.; Sherrill, C. D. *J. Phys. Chem. A* **2006**, *110*, 10656–10668.

(16) Hesselmann, A.; Jansen, G.; Schütz, M. *J. Chem. Phys.* **2005**, *122*, 14103.

(17) Misquitta, A. J.; Szalewicz, K. *J. Chem. Phys.* **2005**, *122*, 214109.

(18) Misquitta, A. J.; Podeszwa, R.; Jeziorski, B.; Szalewicz, K. *J. Chem. Phys.* **2005**, *123*, 214103.

(19) Chalasinski, G.; Szczesniak, M. M. *Mol. Phys.* **1988**, *63*, 205–224.

(20) Cybulski, S. M.; Chalasinski, G.; Moszynski, R. *J. Chem. Phys.* **1990**, *92*, 4357–4363.

(21) Cybulski, S. M.; Lytle, M. L. *J. Chem. Phys.* **2007**, *127*, 141102.

(22) Hesselmann, A. *J. Chem. Phys.* **2008**, *128*, 144112.

(23) Pitonak, M.; Hesselmann, A. *J. Chem. Theory Comput.* **2010**, *6*, 168–178.

(24) Tkatchenko, A.; Distasio, R. A.; Head-Gordon, M.; Scheffler, M. *J. Chem. Phys.* **2009**, *131*, 094106.

(25) Grafova, L.; Pitonak, M.; Rezac, J.; Hobza, P. *J. Chem. Theory Comput.* **2010**, *6*, 2365–2376.

(26) Hohenstein, E. G.; Jaeger, H. M.; Carrell, E. J.; Tschumper, G. S.; Sherrill, C. D. *J. Chem. Theory Comput.* **2011**, *7*, 2842–2851.

(27) Hesselmann, A.; Korona, T. *Phys. Chem. Chem. Phys.* **2011**, *13*, 732–43.

(28) Jenness, G. R.; Karalti, O.; Al-Saidi, W. A.; Jordan, K. D. *J. Phys. Chem. A* **2011**, *115*, 5955–5964.

(29) Karalti, O.; Alfe, D.; Gillan, M. J.; Jordan, K. D. *Phys. Chem. Chem. Phys.* **2012**, *14*, 7846–7853.

(30) Granatier, J.; Pitonak, M.; Hobza, P. *J. Chem. Theory Comput.* **2012**, *8*, 2282–2292.

(31) Huang, Y.; Shao, Y.; Beran, G. J. O. *J. Chem. Phys.* **2013**, *138*, 224112.

(32) Dombroski, J. P.; Taylor, S. W.; Gill, P. M. W. *J. Phys. Chem.* **1996**, *100*, 6272–6276.

(33) Gill, P. M. W.; Adamson, R. D.; Pople, A. C. J. A. *Mol. Phys.* **1996**, *88*, 1005–1009.

(34) Lee, A. M.; Taylor, S. W.; Dombroski, J. P.; Gill, P. M. W. *Phys. Rev. A* **1997**, *55*, 3233–3235.

(35) Gill, P. M. W. *Chem. Phys. Lett.* **1997**, *270*, 193–195.

(36) Adamson, R. D.; Dombroski, J. P.; Gill, P. M. W. *Chem. Phys. Lett.* **1996**, *254*, 329–336.

(37) Adamson, R. D.; Gill, P. M. W. *J. Mol. Struct. (Theochem)* **1997**, *399*, 45–54.

(38) Panas, I. *Chem. Phys. Lett.* **1995**, *245*, 171–177.

(39) Panas, I.; Snis, A. *Theor. Chem. Acc.* **1997**, *97*, 232–239.

(40) Savin, A.; Flad, H.-J. *Int. J. Quant. Chem.* **1995**, *56*, 327–332.

(41) Leininger, T.; Stoll, H.; Werner, H.-J.; Savin, A. *Chem. Phys. Lett.* **1997**, *275*, 151–160.

(42) Gori-Giorgi, P.; Savin, A. *Phys. Rev. A* **2006**, *73*, 032506.

(43) Toulouse, J.; Savin, A.; Flad, H.-J. *Int. J. Quant. Chem.* **2004**, *100*, 1047–1056.

(44) Toulouse, J.; Colonna, F.; Savin, A. *Phys. Rev. A* **2004**, *70*, 062505.

(45) Sharkas, K.; Toulouse, J.; Savin, A. *J. Chem. Phys.* **2011**, *134*, 064113.

(46) Yanai, T.; Tew, D. P.; Handy, N. C. *Chem. Phys. Lett.* **2004**, *393*, 51–57.

(47) Peach, M. J. G.; Cohen, A. J.; Tozer, D. J. *Phys. Chem. Chem. Phys.* **2006**, *8*, 4543–9.

(48) Cohen, A. J.; Mori-Sánchez, P.; Yang, W. *J. Chem. Phys.* **2007**, *126*, 191109.

(49) Iikura, H.; Tsuneda, T.; Yanai, T.; Hirao, K. *J. Chem. Phys.* **2001**, *115*, 3540.

(50) Tawada, Y.; Tsuneda, T.; Yanagisawa, S.; Yanai, T.; Hirao, K. *J. Chem. Phys.* **2004**, *120*, 8425–33.

(51) Janesko, B. G.; Henderson, T. M.; Scuseria, G. E. *Phys. Chem. Chem. Phys.* **2009**, *11*, 443–54.

(52) Weintraub, E.; Henderson, T. M.; Scuseria, G. E. *J. Chem. Theory Comput.* **2009**, *5*, 754–762.

(53) Haunschild, R.; Scuseria, G. E. *J. Chem. Phys.* **2010**, *132*, 224106.

(54) Song, J.-W.; Peng, D.; Hirao, K. *J. Comp. Chem.* **2011**, *32*, 3269–75.

(55) Peverati, R.; Truhlar, D. G. *J. Phys. Chem. Lett.* **2011**, *2*, 2810–2817.

(56) Goldey, M.; Head-Gordon, M. *J. Phys. Chem. Lett.* **2012**, *3*, 3592–3598.

(57) Goldey, M.; Dutoi, A.; Head-Gordon, M. *Phys. Chem. Chem. Phys.* **2013**, *15*, 15869–15875.

(58) Chai, J.-D.; Head-Gordon, M. *J. Chem. Phys.* **2008**, *128*, 084106.

(59) Chai, J.-D.; Head-Gordon, M. *Phys. Chem. Chem. Phys.* **2010**, *10*, 6615–5520.

(60) Goldey, M.; DiStasio, R. A.; Shao, Y.; Head-Gordon, M. *Mol. Phys.* **2014**, *112*, 836–843.

(61) Goldey, M.; Head-Gordon, M. *J. Phys. Chem. B* **2014**, *in press*, 140214030535006.

(62) Stone, A. J. *The Theory of Intermolecular Forces*; Clarendon Press: Oxford, 2002.

(63) Dutoi, A. D.; Head-Gordon, M. *J. Phys. Chem. A* **2008**, *112*, 2110–2119.

(64) Shao, Y. et al. *Phys. Chem. Chem. Phys.* **2006**, *8*, 3172–3191.

(65) Dunlap, B. I. *J. Chem. Phys.* **1983**, *78*, 3140–3142.

(66) Feyereisen, M. W.; Fitzgerald, G.; Komornicki, A. *Chem. Phys. Lett.* **1993**, *208*, 359–363.

(67) Dunning, T. H. *J. Chem. Phys.* **1989**, *90*, 1007–1023.

(68) Weigend, F.; Köhn, A.; Hättig, C. *J. Chem. Phys.* **2002**, *116*, 3175–3183.

(69) Steele, R. P.; Distasio, R. A.; Head-Gordon, M. *J. Chem. Theory Comput.* **2009**, *5*, 1560–1572.

(70) MOLPRO, version 2010.1, a package of ab initio programs, H.-J.Werner, P. J. Knowles, G. Knizia, F. R. Manby, M. Schütz, P. Celani, T. Korona, R. Lindh, A. Mitrushenkov, G. Rauhut, K. R. Shamasundar, T. B. Adler, R. D. Amos, A. Bernhardsson, A. Berning, D. L. Cooper, M. J. O. Deegan, A. J. Dobbyn, F. Eckert, E. Goll, C. Hampel, A. Hesselmann, G. Hetzer, T. Hrenar, G. Jansen, C. Köppel, Y. Liu, A. W. Lloyd, R. A. Mata, A. J. May, S. J. Mchnicholas, W. Meyer, M. E. Mura, A. Nicklass, D. P. O'Neill, P. Palmieri, K. Pflüger, R. Pitzer, M. Reiher, T. Shiozaki, H. Stoll, A. J. Stone, R. Tarroni, T. Thorsteinsson, M. Wang, and A. Wolf. See `http://www.molpro.net`.

(71) Karton, A.; Martin, J. M. L. *Theor. Chem. Acc.* **2006**, *115*, 330–333.

(72) Helgaker, T.; Klopper, W.; Koch, H.; Noga, J. *J. Chem. Phys.* **1997**, *106*, 9639–9646.

(73) Rezac, J.; Riley, K. E.; Hobza, P. *J. Chem. Theory Comput.* **2011**, *7*, 2427–2438.

(74) Jung, Y.; Sodt, A.; Gill, P. M. W.; Head-Gordon, M. *Proc. Nat. Acad. Sci.* **2005**, *102*, 6692–7.

(75) Faver, J. C.; Benson, M. L.; He, X.; Roberts, B. P.; Wang, B.; Marshall, M. S.; Kennedy, M. R.; Sherrill, C. D.; Merz, K. M. *J. Chem. Theory Comput.* **2011**, *7*, 790–797.

(76) Beran, G. J. O.; Nanda, K. *J. Phys. Chem. Lett.* **2010**, *1*, 3480–3487.

(77) Wen, S.; Beran, G. J. O. *J. Chem. Theory Comput.* **2011**, *7*, 3733–3742.

(78) Wen, S.; Beran, G. J. O. *Cryst. Growth Des.* **2012**, *12*, 2169–2172.

(79) Wen, S.; Beran, G. J. O. *J. Chem. Theory Comput.* **2012**, *8*, 2698–2705.

(80) Karamertzanis, P. G.; Day, G. M.; Welch, G. W. A.; Kendrick, J.; Leusen, F. J. J.; Neumann, M. A.; Price, S. L. *J. Chem. Phys.* **2008**, *128*, 244708.

(81) Hongo, K.; Watson, M. A.; Sanchez-Carrera, R. S.; Iitaka, T.; Aspuru-Guzik, A. *J. Phys. Chem. Lett.* **2010**, *1*, 1789–1794.

(82) Freeman, C. M.; Andzelm, J. W.; Ewig, C. S.; Hill, J.-R.; Delley, B. *Chem. Commun.* **1998**, 2455–2456.

(83) Rivera, S. A.; Allis, D. G.; Hudson, B. S. *Cryst. Growth. Des.* **2008**, *8*, 3905–3907.

(84) Marom, N.; DiStasio, R. a.; Atalla, V.; Levchenko, S.; Reilly, A. M.; Chelikowsky, J. R.; Leiserowitz, L.; Tkatchenko, A. *Angew. Chem. Int. Ed.* **2013**, *52*, 6629–32.

(85) Williams, H. L.; Mas, E. M.; Szalewicz, K.; Jeziorski, B. *J. Chem. Phys.* **1995**, *103*, 7374–7391.

(86) Valdes, H.; Pluhackova, K.; Pitonak, M.; Rezac, J.; Hobza, P. *Phys. Chem. Chem. Phys.* **2008**, *10*, 2747–2757.